IET Nanobiotechnology

Research Article

IET Journals
The Institution of Engineering and Technology

Facile synthesis of anisotropic gold nanoparticles and its synergistic effect on breast cancer cell lines

ISSN 1751-8741
Received on 16th October 2019
Revised 24th December 2019
Accepted on 31st January 2020
E-First on 28th February 2020
doi: 10.1049/iet-nbt.2019.0279
www.ietdl.org

Mubarak Jannathul Firdhouse[1] ✉, *Pottail Lalitha*[2]

[1]*Department of Chemistry, Hajee Karutha Rowther Howdia College, Uthamapalayam, Theni, TN 625533, India*
[2]*Department of Chemistry, Avinashilingam Institute for Home Science and Higher Education for Women University, Coimbatore, TN 641043, India*
✉ *E-mail: kfirdhouse@gmail.com*

Abstract: Gold nanoparticles (AuNPs) possess colourful light-scattering properties due to different composition, size and shape. Their unique physical, optical and chemical properties coupled with advantages, have increased the scope of anisotropic AuNPs in various fields. This study reports a green methodology developed for the synthesis of anisotropic AuNPs. The aqueous extracts of *Alternanthera sessilis* (PGK), *Portulaca oleracea* (PAK) and *Sterculia foetida* (SF) with gold ions produced violet, purple and pink coloured AuNPs, respectively, under sonication and room temperature methods revealing the formation of different shapes of AuNPs. The results of TEM analysis of AuNPs confirmed the formation of triangular plate AuNPs of the size 35 nm for PAK extract. Spherical-shaped AuNPs (10–20 nm) were obtained using an extract of PGK. SF extract produced rod, hexagon, pentagon-shaped AuNPs and nanorice gold particles. The cell viability studies of the PGK, PAK and SF-mediated AuNPs on MCF-7 cell lines by MTT assay revealed the cytotoxic activity of AuNPs to depend on the size, shape and the nature of capping agents. The synthesised AuNPs significantly inhibited the growth of cancer cells (MCF-7) in a concentration-dependent manner. The size and shape of these anisotropic AuNPs also reveal its potency to be used as sensors, catalysis, photothermal and therapeutic agents.

1 Introduction

A multidisciplinary outburst of new materials and the manipulation of a structure at the nanoscale level have led to the synthesis of metallic nanoparticles (NPs) [1]. It is the subject of intense investigation from diverse points of view [2]. Nanotechnology plays a crucial role in the organisation of the developed nanoscale structures into predefined superstructures [3]. Gold is a classic noble metal of curiosity, widely superior owing to their stability and ease of use [4]. Its revitalisation in nanotechnology has led to an incomparable increase in its applications in biology, catalysis, optics and many more fields [5]. Gold NPs (AuNPs) possess unique and tunable surface plasmon resonance (SPR) and show advantages in clinical applications over other metallic particles in terms of biocompatibility and photothermal therapy [6]. It has been considered as an important area of research owing to its high chemical and thermal stabilities [7].

In this scenario, herbs have created a revolution symbolising the importance and safety, in contrast to synthetic drugs all over the world. Nearly 20% of the world's population is still using natural products as medicine [8]. Plants are a good source of secondary metabolites which find use in pharmaceutical research. In past years, a large percentage of commercially available new drugs are from natural products. Hence, biological synthesis of products has to be implemented for new findings [9]. The preparation of metal NPs using organisms under mild reaction conditions without the use of hazardous chemicals exploits the environmentally friendly synthesis, which is the most widely, used a bottom-up approach [10].

AuNPs can be synthesised with defined size control and polydispersity by many protocols [11, 12], but the majority of earlier research focus on isotropic spherical particles. Sparse reports are available for the synthesis of anisotropic AuNPs using plant extracts. NPs of varying composition, size, shape and architecture have been explored as photothermal agents [13, 14] and radiosensitiser agents [15] in the field of cancer nanomedicine. However, anisotropic particles are particularly interesting, because the decreased symmetry of such particles often leads to new and unusual chemical and physical properties. The anisotropy of these non-spherical, hollow and nanoshell AuNP structures is the source of the plasmon absorption in the visible region as well as in the near-infrared (NIR) region [16].

A reliable and controllable measure to synthesise NPs is sonication, as it involves the energy generated via the production of sound waves. Ultrasounds with frequencies as high as 20 000 Hz are very effective energy carriers and ensure a very easy breakdown of bulk precursors to yield nanoparticles with specific applications and morphology. The mechanism behind ultrasound is acoustic cavitation's. The extreme conditions generated during the bubble collapse aid in NPs synthesis [17]. Citrus lemon, citrus pineapple, citrus grapes and citrus orange juice extracts treated with gold ions produced spherical AuNPs by sonication method [18]. AuNPs of the size 5–75 nm were synthesised using an ethanolic leaf extract of *Andrographis paniculata* in <2 min of sonication [19].

In this work, a simple, green and economic methodology has been developed for the synthesis of anisotropic AuNPs using *Alternanthera sessilis* (PGK), *Portulaca oleracea* (PAK) and *Sterculia foetida* (SF) extracts under sonication and room temperature conditions, respectively, compared to other synthesis methods reported earlier. Literature reports revealed cytotoxicity of AuNPs to depend on the shape and size of the AuNPs. In order to study the effect of shape and size of AuNPs on cytotoxicity, the different coloured AuNPs produced using PGK, PAK and SF extracts were taken up in the cell viability study on MCF-7 cell lines.

2 Materials and methods

The fresh parts of the selected plants (PGK, PAK, SF (20 g)) were weighed, washed thrice with distilled water and cut into fine pieces, and then 100 ml Millipore water was added and boiled for 5 min in a 500 ml Erlenmeyer flask. The prepared solutions were filtered using Whatman filter paper No. 42 to remove the plant debris, sonicated for 15 min and refrigerated at −4°C for further studies. This filtrate obtained (designated as aqueous extract) was

© The Institution of Engineering and Technology 2020

Fig. 1 *Photograph of different colours of anisotropic AuNPs*

used within a week for the synthesis of NPs to avoid the annihilation of phytoconstituents. The stock solution of chloroauric acid ($HAuCl_4$) (3 mM) was prepared by dissolving the required amount of $HAuCl_4$ in Millipore water separately and the subsequent different volumes for the synthesis of AuNPs were taken from the stock solution.

2.1 Synthesis of anisotropic AuNPs

The different synthesis methods were optimised and adopted to produce biogenic AuNPs of different shapes viz., spherical, nanotriangular plate, nanorice, hexagon, icosahedron etc., which have real applications in practice.

2.1.1 Spherical AuNPs: Aqueous extracts of *A. sessilis* (4 ml) were treated with a constant volume of gold ions (1 ml) separately to yield rapid formation of spherical AuNPs without agglomeration under room temperature. The completion of the violet coloured nanogold formation was noted within 10 min.

2.1.2 Triangular-plate AuNPs: The sonic wave-assisted synthesis was adopted to produce nanotriangles and hexagon shape AuNPs using *P. oleracea* (2 ml) and 1 ml gold chloride solution. Purple coloured AuNPs were formed within 15 min of sonication.

2.1.3 Icosahedron and hexagon-shaped AuNPs: SF extract (5 ml) and gold ions (3 ml) were mixed and kept at room temperature for 90 min to synthesise icosahedron, hexagon and nanotriangles.

2.1.4 Gold nanorice: Gold chloride solution (3 ml) and aqueous extract of *S. foetida* (5 ml) was mixed and sonicated for 20 min to get nanorice.

2.2 Purification of biosynthesised AuNPs

The biosynthesised AuNPs were separated from the bulk reaction mixture using a centrifugator (Spectrofuge 7M). The residues obtained were redispersed into Millipore water with repeated centrifugation. The supernatant solutions were refrigerated for characterisation and further experiments.

2.3 Characterisation of the synthesised AuNPs

UV–vis spectroscopy, X-ray diffraction (XRD) etc. are the spectroscopic techniques intended as basic tools for the characterisation of NPs. Electron microscopy techniques are very useful in ascertaining the overall shape of metal NPs.

2.3.1 UV–vis spectroscopy: UV–vis spectroscopy implies the spectroscopic properties of NPs and provides size distribution by means of fitting the position of SPR band of simple wavelength function. It is the diagnostic tool widely used for the study of NPs formation. The formation and completion of AuNPs were characterised by UV–vis spectroscopy using a double beam spectrophotometer 2202-(SYSTRONICS). The scanning range of the samples was 200–800 nm at a scan speed of 480 nm/min. The spectrophotometer was equipped with 'Hitachi UV lamp-F8T5 Software' to record and analyse data. Baseline calibration of the spectrophotometer was carried out by using a blank reference.

2.3.2 XRD analysis: A drop coated film of synthesised AuNPs on a glass substrate was characterised using X'pert Pro X-ray diffractometer with a CuKα radiation ($\lambda = 1.54060$ Å) monochromatic filter operated at 45 kV and 30 mA over the range of $2\theta = 10°–80°$ [scanning rate 2°/min].

2.3.3 Fourier transform infrared (FTIR) spectroscopy: FTIR analysis assists in the identification of organic functional groups responsible for the reduction of metal ions to metal NPs. The aqueous solution of biosynthesised AuNPs after centrifugation was analysed by FTIR spectrum (Bruker FTIR Tensor-27).

2.3.4 Transmission electron microscopy (TEM): TEM offers a high resolution of particle size, shape and also dispersity. The nanodimension of the synthesised AuNPs was established through recording TEM images using FEI's Tecnai G2 Transmission Electron Microscope. The imaging of the sonicated AuNPs was enabled by depositing a few drops of suspension on a carbon film 200 mesh, a copper grid of 2.8 mm diameter and the solvent was dried in a desiccator at room temperature prior to recording TEM.

2.4 Anticancer activity of AuNPs against MCF-7 cell line

The MCF-7 cell was plated in 96 well plates at a concentration of 1 × 104 cells/well. After 24 h, cells were washed twice with 100 µl of serum-free medium and starved for an hour at 37°C. After starvation, cells were treated with different concentrations of AuNPs (12.5, 25, 50, 100, 200 µg/ml) for 24 h. At the end of the treatment period, the medium was aspirated and serum-free medium containing MTT (0.05 mg/ml) was added and incubated for 4 h at 37°C in a CO_2 incubator. The MTT containing medium was then discarded and the cells were washed with PBS (200 µl). The crystals were then dissolved by adding 100 µl of DMSO and this was mixed properly. Spectrophotometrical absorbance of the purple, blue formazan dye was measured in a microplate reader at 570 nm. Cytotoxicity was determined using Graph pad prism5 software. The assay is based on the reduction of soluble yellow tetrazolium salt to insoluble purple formazan crystals by metabolically active cells. Only live cells are able to take up the tetrazolium salt. The enzyme (succinate dehydrogenase) present in the mitochondria of the liver cells is able to convert internalised tetrazolium salt to formazan crystals, which are purple in colour.

3 Results and discussion

Photograph of different colours of anisotropic AuNPs synthesised using PAK, PGK and SF extracts is shown in Fig. 1.

3.1 Spherical AuNPs

A. sessilis extract and gold ions produced violet colour AuNPs at room temperature in 15 min. Absorption spectra of AuNPs formed using PGK extract exhibit absorbance maxima at 560 nm (Fig. 1*a*). A shift in SPR bands towards longer wavelengths (blue shift) and broad shape indicate the formation of larger NPs. TEM micrographs (Fig. 2*a*) portray PGK-AuNPs to be spherical and size <20 nm. The SPR band at 565 nm is that of the spherical NPs with the slightly ellipsoidal shape of the cluster on the surface. The distinct blue shift is attributed to quantum size effects that come into play when the particle size becomes comparable to the mean free path of electrons in the metal [20–23].

3.2 Triangular-plate AuNPs

Purple coloured AuNP's were formed after 5–15 min sonication of PAK with gold chloride solution. PAK-mediated AuNPs (Fig. 1*b*) reveal the presence of bands at 540 and 570 nm, with a difference in their intensity. According to Mie theory, spherical AuNPs exhibit a single SPR band, whereas anisotropic particles may show

© The Institution of Engineering and Technology 2020

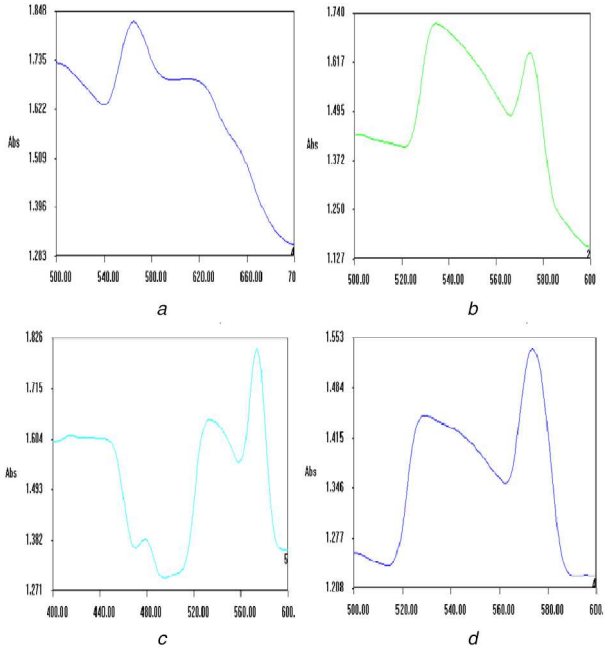

Fig. 2 *UV–visible spectra of nanogold synthesised using* ***(a)*** PGK, ***(b)*** PAK, ***(c)*** *and* ***(d)*** SF extracts

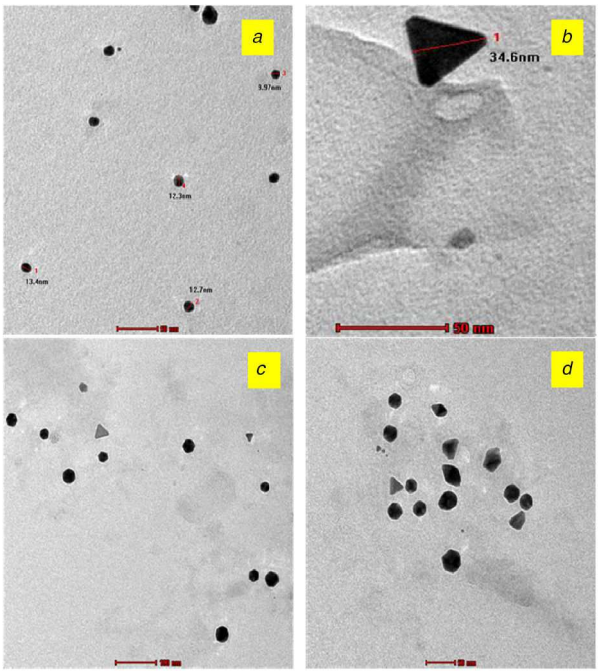

Fig. 3 *TEM micrographs of nanogold synthesised using* ***(a)*** PGK, ***(b)*** PAK, ***(c)*** *and* ***(d)*** SF extracts

2–3 SPR bands [24]. The SPR band of AuNPs shows an absorption peak at 540 nm resulting in out-of-plane quadrupole resonance. The absorption band in the region of 620–1100 nm is a result if in-plane dipole resonance [25]. In this study, the SPR bands noted in Fig. 1*b* disclose the presence of different shapes of AuNPs.

The fabrication of the triangular plate was achieved by sonication method using PAK extract. High dispersion produced in the sonication method may be one of the contributing factors in addition to the constituents like alkaloids, tannins and terpenoids present in the PAK extract for the formation of triangular plate AuNPs. TEM micrographs confirm the formation of a triangular plate with smooth edges in PAK-mediated AuNPs of size 35 nm (Fig. 2*b*).

Triangular AuNPs, along with some sphere and hexagonal shapes were formed using endophytic fungi *Aspergillus clavatus* and exploitable in a myriad of diagnostic and therapeutic applications [26]. Aqueous extract of *Sargassum myriocystum* produced stable polydispersed (triangular and spherical) AuNPs with an average size of 15 nm at 76°C after 15 min [27]. These gold nanotriangles with unique and highly anisotropic planar shapes might find applications in photonics, optoelectronics, optical sensing [28], bioimaging and biolabelling [29].

Similar observations were noted in the aggregation and rearrangement of smaller triangle-shaped nanogold particles using lemongrass extracts. The authors have reported the process to be kinetically driven with a low rate of reduction of metal ions which facilitate the anisotropic AuNPs even at room temperature [30]. The percentage of gold nanotriangles compared to spherical particles was appreciably abridged at high temperature, whereas nanotriangle formation was noted at low temperatures [31].

Extremely flat morphology is the key feature of gold nanotriangles which provides high thermal contact with tumour cells, thereby reducing exposure time. These unique optical properties of gold nanotriangles make them a promising candidate for photothermal treatment and hyperthermia of tumours. Hence, gold nanotriangles are considered to be the best option in comparison to gold nanorods and gold nanospheres for cancer treatment [32]. In this work, the biosynthesis route has led to the formation of triangle-shaped AuNPs by sonication method in lesser time (5–15 min) compared to previous reports. These AuNPs may find promising applications in sensors, diagnostic and cancer therapeutic applications.

3.3 Icosahedron and hexagon-shaped AuNPs

SF extract and gold ions produced pink colour AuNPs at room temperature in 90 min. Two sharp bands at 520 and 570 nm were noted for SF-AuNPs. The intensity (peak height) of a band at 570 nm is higher compared to the band at 520 nm implying the formation of anisotropic nanogold other than sphere shape (Fig. 2*c*). Hexagon, pentagon and triangle-shaped nanogold are clearly depicted in the TEM image of SF-AuNPs (Fig. 3*c*). The results of UV–vis spectrum were analogous to TEM images of SF-AuNPs.

Special geometrical structures such as the triangle and hexagon AuNPs of the size 50–80 nm were obtained using leaf extract of *Dalbergia sissoo* which find applications in optical sensors and NIR absorbers [30]. Cocoa extract-mediated synthesis produced anisotropic AuNPs by an aqueous route which is cytocompatible and suitable for photothermal therapy [15]. Various morphologies from nanotriangles to nanohexagon with more spherical-shaped nanogold were synthesised using *Gnidia glauca* flower extract [32]. Tannins and saponins are the major metabolites present in the SF extract probably attribute to the production of the hexagon and pentagon-shaped AuNPs. Hence the biosynthesised anisotropic AuNPs may be used in developing sensors and in photothermal therapy.

3.4 Gold nanorice

Sonication of a mixture of gold ions (3 ml) and aqueous extract (5 ml) of SF for 20 min produced purple colour AuNPs. Fig. 1*d* reveals the presence of sharp SPR bands at 560, 620 and 640 nm which corresponds to polyshaped AuNPs. A significant difference in the shape of nanorice compared to other anisotropic nanogold is noted in the TEM image (Fig. 3*d*). This is the first report on nanorice gold particles using plant extracts.

The name ‘Nanorice’ was coined due to the dielectric core-metallic shell prolate spheroid shape and its outstanding resemblance to a grain of rice. This geometry possesses far greater structural tunability than either a nanorod or a nanoshell [33]. Gold nanorice synthesised by a facile method showed much higher catalytic activity for CO oxidation than multiply twinned particles of gold enclosed by {111} facets at temperatures below 300°C [34]. Rice-shaped gold nanostructures produced using an aqueous extract of the eggshells of *Anas platyrhynchos* was utilised for the removal of a toxic Eosin Y dye by photodegradation [35].

The production of nanorice gold particles by sonication method using SF extract was achieved in this work. The higher catalytic activity of gold nanorice is reported in the literature and hence the

© The Institution of Engineering and Technology 2020

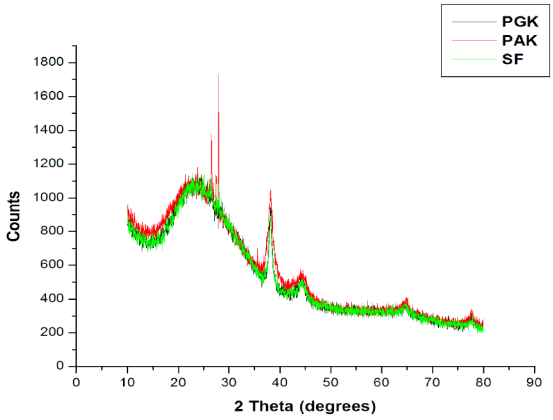

Fig. 4 *XRD patterns of synthesised AuNPs using PGK, PAK and SF extracts*

Table 1 IR frequencies of the synthesised AuNPs

S. no	Plants	AuNP's –IR frequencies, cm^{-1}	Functional groups
1.	PAK	3345, 1667	−NH or −OH, C = O CN triple bond
2.	PGK	3334, 1637	−NH or −OH CC or CN
3.	SF	3344, 3335, 1633, 1503	O–H, N–H, C = O, N–O stretching

Table 2 Results of % cell inhibition of PGK-AuNPs against MCF-7 cell lines

Concentration, µg/ml	% Cell inhibition
12.5	1.57
25	7.21
50	22.98
100	30.39
200	46.10

Table 3 Results of cell viability assay of biosynthesised AuNPs against MCF-7 cell lines

Concentration, µg/ml	% Cell viability of AuNPs		
	PAK-AuNPs	PGK-AuNPs	SF-AuNPs
12.5	102.10	98.43	100.88
25	100.33	92.79	100.33
50	98.50	77.02	87.62
100	94.08	69.61	76.81
200	90.82	53.90	69.00

Table 4 Results of cell inhibition of the biosynthesised AuNPs at 200 µg/ml concentration

Plant-mediated AuNPs	Colour	Shape	Cell inhibition, %
PAK-AuNPs	purple	triangle, spherical	9.18
PGK-AuNPs	violet	spherical	46.10
SF-AuNPs	pink	triangular plate	31

biosynthesised SF-AuNPs are anticipated to be of use in catalytic applications.

3.5 XRD analysis of AuNPs

The XRD patterns of AuNPs exhibit several size-dependent features leading to an irregular peak position, height and width. The XRD patterns of the AuNPs synthesised using the aqueous extract of PGK, PAK and SF are given in Fig. 4. The diffraction angles at 38°, 44°, 64° and 77° corresponds to the (111), (200), (220) and (311) Bragg's reflection of fcc lattice, respectively. The XRD patterns of these AuNPs shows highest intensities for the (111) peak corresponding to $2\theta = 38°$ compared to (200) and (220) peaks. The high intensity of the (111) peak indicates the formation of anisotropic AuNPs (Fig. 4). The anisotropic nature, mainly triangular and hexagonal shapes of AuNPs of (111) orientation, are reported in the XRD analysis of AuNPs synthesised by Fragoon *et al.* [36]. The crystal structure of the highly faceted particles consists of mostly {111} surfaces as particle size increases, for the pentagonal- and hexagonal-shaped AuNPs synthesised using sodium dodecyl sulphate by seeding growth approach as revealed by both TEM and XRD results in the research work of Kuo *et al.* [37].

3.6 FTIR analysis of AuNPs

The FTIR spectral data of the synthesised AuNPs are given in Table 1. The IR frequencies of the synthesised nanogold using PGK, PAK and SF extracts reveal the presence of −NH or −OH, C = O, C–H, CC and CN triple bond functional groups that are responsible for the reduction of gold ions. These groups find the source in the plant extracts which have been used as capping agents. The FTIR spectra of the synthesised AuNPs show the absence or shift of certain IR frequencies revealing the interaction of functional groups with the metal ions and role as reducing agents.

3.7 Antiproliferative effect of AuNPs against MCF-7 cancer cell lines

The AuNPs synthesised using PGK extract was studied for its anticancer activity against MCF-7 cancer cell lines. MTT assay of PGK-AuNPs revealed (Table 2) increase in the concentration of PGK-AgNPs (12.5–100 µg/ml) increase the % cell inhibition from 1.6 to 30%. Since only 30% inhibition was observed, the dosage of PGK-AuNPs was doubled to 200 µg/ml. This resulted in 46% inhibition compared to PGK-AuNPs. PGK-AuNPs did not show much anticancer potential. The study (Table 2) also revealed the non-toxic nature of AuNPs evidenced by the presence of viable cells. The literature reports revealed cytotoxicity of AuNPs to depend on the shape and size of the AuNPs. In order to study the effect of shape and size of AuNPs on cytotoxicity, the different coloured AuNPs produced using PGK, PAK and SF extracts were taken up for the cell viability study on MCF-7 cell lines.

3.8 Percentage cell viability of anisotropic AuNPs against MCF-7 cancer cell lines

The cell viability assay was carried out for the biosynthesised AuNPs against Human Breast (MCF-7) cancer cell lines via MTT assay at concentrations ranging from 12.5 to 200 µg/ml for 48 h exposure. The concentration-dependent toxic effect on cancer cells upon exposure to AuNPs is given in Table 3. The viable cells decrease as the concentration of the PGK-mediated AuNPs increases confirms the cytotoxic activity of these AuNPs.

The biosynthesised PGK-AuNPs showed enhanced inhibition of cancer cells proliferation compared to PAK and SF-mediated AuNPs (Table 3). The presence of anticancer molecules in its extract and the size and shape of the biosynthesised AuNPs governs the cytotoxic activity. From Table 4, it is clear that the spherical-shaped AuNPs (PGK-AuNPs) showed nearly 50% cell inhibition at 200 µg/ml concentration. PAK-AuNPs and SF-AuNPs possess less cytotoxic activity, even at the same concentration (200 µg/ml), which may be attributed to the triangular shape of size 20–40 nm. SF-AuNPs exhibit slightly higher inhibition (31%) due to the presence of monodispersed triangular AuNPs compared to PAK-AuNPs (9%) which are both spherical- and triangular-shaped nanoparticles. The competitive behaviour between the spherical- and triangular-shaped AuNPs may be the reason for the less inhibition of MCF-7 cancer cells than other AuNPs.

Fig. 5 shows the cytomorphological changes like cancer cell membrane lyses and coiling occurring at 200 µg/ml concentration of AuNPs synthesised using PAK, SF and PGK extracts on MCF-7

© The Institution of Engineering and Technology 2020

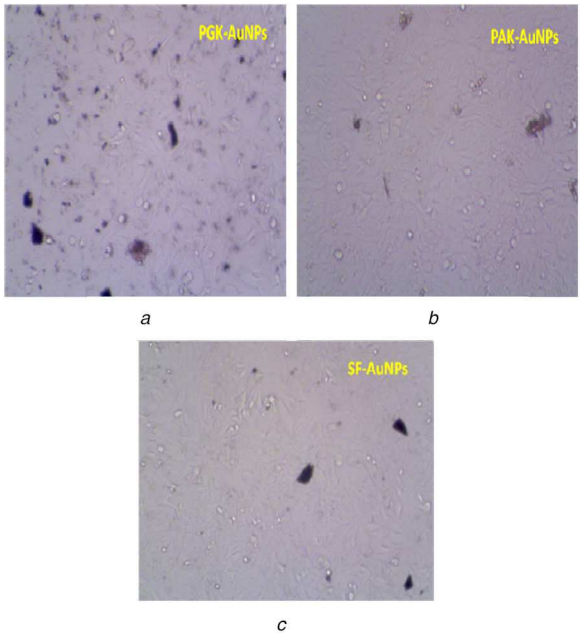

Fig. 5 *Cytomorphological changes and growth inhibition of AuNPs synthesised using PGK*
(a) PAK, ***(b)*** SF, ***(c)*** extracts on MCF-7 cell lines at 200 µg/ml

cell lines. The results suggest the anticancer activity of the PGK mediated AuNPs to be due to the presence of anticancer molecules present in these extracts.

PAK extract reveals the presence of alkaloids, flavonoids, tannins, terpenoids, saponins, glycosides and proteins. Glycosides, proteins, saponins and flavonoids are seen in PGK and SF extracts. All the three extracts revealed the presence of flavonoids, which may be one of the contributing factors for the anticancer activity. The limited inhibition of cell proliferation observed in PAK and SF-mediated AuNPs may be due to the competitive behaviour of the metabolites as capping agents on the synthesised AuNPs, which influence its stability. The significant anticancer properties observed in flavonoids may be due to Frank apoptosis [38].

The ability of mitochondrial dehydrogenase enzyme from viable cells to cleave the tetrazolium rings of the pale yellow MTT to form dark blue formazan crystals attributed to the cytotoxic activity to the cancer cells treated with AuNPs [39]. The nuclear fragmentation in cancer cells was noted after the addition of AuNPs in the previous literature [40, 41]. Meat-ball like AuNPs developed using green tea extract under microwave irradiation are reported to be biocompatible up to 500 µg/ml against MCF-7 and HeLa cell lines [42]. The ethanolic extract of *Fagopyrum esculentum* produced AuNPs showed excellent viability up to 100 µmol/l concentrations against human HeLa, MCF-7 and IMR-32 cancer cell lines [43]. The anticancer study of PGK-AgNPs revealed complete apoptosis (94%) at 25 µl/ml for prostate cancer cell lines (PC-3) [44], whereas 99% growth inhibition was obtained for breast cancer cell lines (MCF-7) [45] using MTT assay. Flower-shaped AuNPs synthesised using *Kedrostis foetidissima* showed almost 96% viability for bone cancer cell lines (MG-63) after exposure to 200 µg/ml concentration [46]. The previous literature revealed cytotoxicity of AuNPs depends upon the shape and size of the AuNPs.

In this work, less inhibition of MCF-7 cancer cells obtained for the biosynthesised AuNPs indicates its biocompatibility. Hence the difference in the percentage cell inhibition obtained for these AuNPs and its toxicity behaviour mainly imparts on their shape and size. Thus, it can be used in cancer therapy and drug delivery applications. The results of the cell viability study of the biosynthesised AuNPs reveal the cytotoxic activity of AuNPs to depend on the size, shape and the nature of capping agents. The interaction of spherical-shaped AuNPs with cancer cell membrane may enhance the permeability, whereas it is depressed for the triangle-shaped AuNPs. This insists smaller size NPs to occupy more surface area than larger ones.

The phytoconstituents will upsurge the stability of the synthesised NPs and enhance the anticancer activity. Hence the ingredients from the plants are the contributing factors for biological and pharmacological applications. In the case of other applications like sensor and catalysis, the capping agents are removed because the size and shape of the NPs play a vital role.

4 Conclusion

The green methodology was developed for the synthesis of anisotropic AuNPs using PGK, PAK and SF extracts. The SPR band varies for the synthesised AuNPs indicating the formation of different shapes and sizes. The results of TEM analysis of AuNPs confirmed the formation of triangular plate AuNPs of size 20–30 nm for PAK and SF produced rod, hexagon, pentagon-shaped and nanorice AuNPs. These anisotropic AuNPs may be used as sensors, catalysis, photothermal, diagnostic and therapeutic agents. The results of the cell viability studies of the PGK, PAK and SF-mediated AuNPs on MCF-7 cell lines revealed the cytotoxic activity of AuNPs to depend on the size, shape and the nature of capping agents. The superior anticancer or cytotoxic activity of the PGK-AgNPs may be due to the spherical shape and smaller particle size (10–20 nm) of PGK-AgNPs as confirmed from TEM analysis.

6 Acknowledgments

The authors thank the Avinashilingam Institute for Home Science and Higher Education for Women, Coimbatore, Tamil Nadu, for providing research facilities, TNAU, Coimbatore for recording TEM and KMCH College of Pharmacy for certifying anticancer activity of test samples.

7 References

[1] Min, Y., Akbulut, M., Kristiansen, K., *et al.*: 'The role of interparticle and external forces in nanoparticles assembly', *Nat. Mater.*, 2008, **7**, pp. 527–538
[2] Toshima, N., Yonezawa, T.: 'Bimetallic nanoparticles – novel materials for chemical and physical applications', *New J. Chem.*, 1998, **22**, pp. 1179–1201
[3] Iravani, S.: 'Green synthesis of metal nanoparticles using plants', *Green Chem.*, 2011, **13**, pp. 2638–2650
[4] Desireddy, A., Conn, B.E., Guo, J., *et al.*: 'Ultrastable silver nanoparticles', *Nature*, 2013, **501**, pp. 399–402
[5] Mishra, B., Patel, B.B., Tiwari, S.: 'Colloidal nanocarriers: a review on formulation technology, types and applications toward targeted drug delivery', *Nanomed. Nanotechnol. Biol. Med.*, 2010, **6**, pp. 9–24
[6] Abadeer, S.N., Murphy, C.J.: 'Recent progress in cancer thermal therapy using gold nanoparticles', *J. Phys. Chem. C*, 2016, **120**, pp. 4691–4716
[7] Naraginti, S., Sivakumar, A.: 'Eco-friendly synthesis of silver and gold nanoparticles with enhanced bactericidal activity and study of silver catalyzed reduction of 4-nitrophenol', *Spectrochim. Acta A, Mol. Biomol. Spectrosc.*, 2014, **15**, pp. 357–362
[8] Cragg, G.M., Newman, D.J., Snader, K.M.: 'Natural products in drug discovery and development', *J. Nat. Prod.*, 1997, **60**, pp. 52–60
[9] Tiwari, S.: 'Plants: a rich source of herbal medicine', *J. Nat. Prod.*, 2008, **1**, pp. 27–35
[10] Mittal, A.K., Chisti, Y., Banerjee, U.C.: 'Synthesis of metallic nanoparticles using plant extracts', *Biotechnol. Adv.*, 2013, **31**, pp. 346–356
[11] Hu, M., Chen, J., Li, Z., *et al.*: 'Gold nanostructures: engineering their plasmonic properties for biomedical applications', *Chem. Soc. Rev.*, 2006, **35**, pp. 1084–1094
[12] Millstone, J.E., Hurst, S.J., Métraux, G.S., *et al.*: 'Colloidal gold and silver triangular nanoprisms', *Small*, 2009, **5**, pp. 646–664
[13] Bucharskaya, A., Maslyakova, G., Terentyuk, G., *et al.*: 'Towards effective photothermal/photodynamic treatment using plasmonic gold nanoparticles', *Int. J. Mol. Sci.*, 2016, **17**, pp. 1–26
[14] Popovtzer, A., Mizrachi, A., Motiei, M., *et al.*: 'Actively targeted gold nanoparticles as novel radiosensitizer agents: an in vivo head and neck cancer model', *Nanoscale*, 2016, **8**, pp. 2678–2685
[15] Fazal, S., Jayasree, A., Sasidharan, S., *et al.*: 'Green synthesis of anisotropic gold nanoparticles for photothermal therapy of cancer', *ACS Appl. Mater. Interfaces*, 2014, **6**, pp. 8080–8089
[16] Li, N., Zhao, P., Astruc, D.: 'Anisotropic gold nanoparticles: synthesis, properties, applications, and toxicity', *Angew. Chem., Int. Ed.*, 2014, **53**, pp. 1756–1789
[17] Malik, P., Shankar, R., Malik, V., *et al.*: 'Green chemistry based benign routes for nanoparticle synthesis', *J. Nanoparticle*, 2014, **Article ID 30242**, p. 6
[18] Dhanemozhi, A.C., Chitra, D.: 'Synthesis of gold nanoparticles with fruit extract'. Proc. of 3rd World Conf. on Applied Sciences, Engineering & Technology, Kathmandu, Nepal, 2014, pp. 572–575, ISBN 13: 978-81-930222-0-7
[19] Babu, P.J., Saranya, S., Sharma, P., *et al.*: 'Gold nanoparticles: sonocatalytic synthesis using ethanolic extract of *Andrographis paniculata* and

© The Institution of Engineering and Technology 2020

functionalization with polycaprolactone-gelatin composites', *Front. Mater. Sci.*, 2012, **6**, pp. 236–249
[20] El-Brolossy, T.A., Abdallah, T., Mohamed, M.B., *et al.*: 'Shape and size dependence of the surface plasmon resonance of gold nanoparticles studied by photoacoustic technique', *Eur. Phys. J. Spec. Top.*, 2008, **153**, pp. 361–364
[21] Ringe, E., Langille, M.R., Sohn, K., *et al.*: 'Plasmon length: a universal parameter to describe size effects in gold nanoparticles', *J. Phys. Chem. Lett.*, 2012, **3**, pp. 1479–1483
[22] Myroshnychenko, V., Rodríguez-Fernandez, J., Pastoriza-Santos, I., *et al.*: 'Modelling the optical response of gold nanoparticles', *Chem. Soc. Rev.*, 2008, **37**, pp. 1792–1805
[23] Palomba, S., Novotny, L., Palmer, R.E.: 'Blue-shifted plasmon resonance of individual size selected gold nanoparticles', *Opt. Commun.*, 2008, **281**, pp. 480–483
[24] Mie, G.: 'Articles on the optical characteristics of turbid tubes, especially colloidal metal solutions', *Ann. Phys. (Berlin)*, 1908, **25**, pp. 377–445
[25] Nikoobakht, B., Wang, J., El-Sayed, M.A.: 'Surface-enhanced Raman scattering of molecules adsorbed on gold nanorods: off-surface plasmon resonance condition', *Chem. Phys. Lett.*, 2002, **366**, pp. 17–23
[26] Verma, V.C., Singh, S.K., Solanki, R., *et al.*: 'Biofabrication of anisotropic gold nanotriangles using extract of endophytic *Aspergillus clavatus* as a dual functional reductant and stabilizer', *Nanoscale Res. Lett.*, 2011, **6**, pp. 1–7
[27] Dhas, T.S., Kumar, V.G., Abraham, L.S., *et al.*: '*Sargassum myriocystum* mediated biosynthesis of gold nanoparticles', *Spectrochim. Acta A, Mol. Biomol. Spectrosc.*, 2012, **99**, pp. 97–101
[28] Ankamwar, B., Damie, C., Ahmad, A., *et al.*: 'Biosynthesis of gold and silver nanoparticles using *Emblica officinalis* fruit extract, their phase transfer and transmetallation in an organic solution', *J. Nanosci. Nanotechnol.*, 2005, **5**, pp. 1665–1671
[29] Sujathadevi, P., Banerjee, S., Chowdhury, S.R., *et al.*: 'Eggshell membrane: a natural biotemplate to synthesize fluorescent gold nanoparticles', *RSC Adv.*, 2012, **2**, pp. 11578–11585
[30] Singh, C., Baboota, R.K., Naik, P.K., *et al.* 'Biocompatible synthesis of silver and gold nanoparticles using leaf extract of *Dalbergia sissoo*', *Adv. Mater. Lett.*, 2012, **3**, pp. 279–285
[31] Dharmatti, R., Phadke, C., Mewada, A., *et al.*: 'Biogenic gold nanotriangles: cargos for anticancer drug delivery', *Mater. Sci. Eng. C*, 2014, **44**, pp. 92–98
[32] Ghosh, S., Patil, S., Ahire, M., *et al.*: '*Gnidia glauca* flower extract mediated synthesis of gold nanoparticles and evaluation of its chemocatalytic potential', *J. Nanobiotechnol.*, 2012, **10**, pp. 1–9
[33] Wang, H., Brandl, D.W., Le, F., *et al.*: 'Nanorice: a hybrid plasmonic nanostructures', *Nano Lett.*, 2006, **6**, pp. 827–832
[34] Zheng, Y., Tao, J., Liu, H., *et al.*: 'Facile synthesis of gold nanorice enclosed by high index facets and its application for CO oxidation', *Small*, 2011, **7**, pp. 2307–2312
[35] Sinha, T., Ahmaruzzaman, M.: 'A novel green and template free approach for the synthesis of gold nanorice and its utilization as a catalyst for the degradation of hazardous dye', *Spectrochim. Acta A, Mol. Biomol. Spectrosc.*, 2015, **142**, pp. 266–270
[36] Fragoon, A., Li, J., Zhu, J., *et al.*: 'Biosynthesis of controllable size and shape gold nanoparticles by blackseed (*Nigella sativa*) extract', *J. Nanosci. Nanotechnol.*, 2012, **3**, pp. 2337–2345
[37] Kuo, C., Chiang, T., Chen, L., *et al.*: 'Synthesis of highly faceted pentagonal- and hexagonal-shaped gold nanoparticles with controlled sizes by sodium dodecyl sulphate', *Langmuir*, 2004, **20**, pp. 7820–7824
[38] Selim, M.E., Hendi, A.A.: 'Gold nanoparticles induce apoptosis in MCF-7 human breast cancer cells', *Asian Pac. J. Cancer Prev.*, 2012, **13**, pp. 1617–1620
[39] Dhas, T.S., Kumar, V.G., Karthick, V., *et al.*: 'Biosynthesis of gold nanoparticles using *Sargassum swartzii* and its cytotoxicity effect on HeLa cells', *Spectrochim. Acta A Mol. Biomol Spectrosc.*, 2014, **133**, pp. 102–106
[40] Kang, B., Mackey, M.A., El-Sayed, M.A.: 'Nuclear targeting of gold nanoparticles in cancer cells induces DNA damage, causing cytokinesis arrest and apoptosis', *J. Am. Chem. Soc.*, 2010, **132**, pp. 1517–1519
[41] Guo, H., Qian, H., Idris, N.M., *et al.*: 'Singlet oxygen-induced apoptosis of cancer cells using upconversion fluorescent nanoparticles as a carrier of photosensitizer', *Nanomedicine'*, 2010, **6**, pp. 486–495
[42] Wu, S., Zhou, X., Yang, X., *et al.*: 'A rapid green strategy for the synthesis of Au 'meatball'-like nanoparticles using green tea for SERS applications', *J. Nanoparticle Res.*, 2014, **16**, pp. 1–13
[43] Babu, P.J., Sharma, P., Kalita, M.C., *et al.*: 'Green synthesis of biocompatible gold nanoparticles, using *Fagopyrum esculentum* leaf extract', *Front. Mater. Sci.*, 2011, **5**, pp. 379–387
[44] Firdhouse, M.J., Lalitha, P.: 'Biosynthesis of silver nanoparticles using the extract of *Alternanthera sessilis* – antiproliferative effect against prostate cancer cells', *Cancer Nano.*, 2013, **4**, pp. 137–143
[45] Firdhouse, M.J., Lalitha, P.: 'Apoptotic efficacy of biogenic silver nanoparticles on human breast cancer MCF-7 cell lines', *Prog Biomater.*, 2015, **4**, pp. 113–121
[46] Firdhouse, M.J., Lalitha, P.: 'Flower-shaped gold nanoparticles synthesized using *Kedrostis foetidissima* and their antiproliferative activity against bone cancer cell lines', *Int. J. Ind. Chem.*, 2016, **7**, (4), pp. 347–358

© The Institution of Engineering and Technology 2020